THE JOURNAL OF PHYSICAL CHEMISTRY B
A JOURNAL OF THE AMERICAN CHEMICAL SOCIETY

pubs.acs.org/JPCB

Article

Systematic Parameterization of Ion−Surfactant Interactions in Dissipative Particle Dynamics Using Setschenow Coefficients

Ennio Lavagnini, Joanne L. Cook, Patrick B. Warren, and Christopher A. Hunter*

Cite This: *J. Phys. Chem. B* 2022, 126, 2308−2315

Read Online

ACCESS | Metrics & More | Article Recommendations

ABSTRACT: Dissipative particle dynamics (DPD) simulations of nonionic surfactants with an added salt show that the Setschenow relationship is reproduced; that is, the critical micelle concentration is log-linearly dependent on the added salt concentration. The simulated Setschenow coefficients depend on the DPD bead−bead repulsion amplitudes, and matching to the experimentally determined values provides a systematic method to parameterize the interactions between salt ion beads and surfactant beads. The optimized ion-specific interaction parameters appear to be transferrable and follow the same trends as the empirical Hofmeister series.

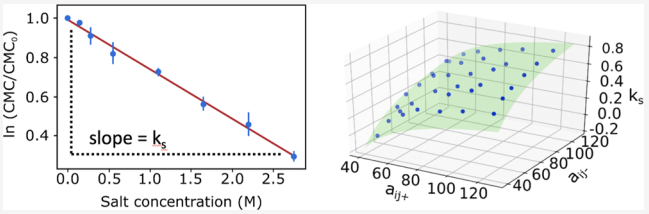

INTRODUCTION

The presence of ions in a solution affects numerous chemical and biophysical phenomena. The magnitude of these effects often follow ion-specific trends such as the Hofmeister series,[1] which was initially introduced to rank the propensity of salts to decrease the solubility of proteins (salting out) and was subsequently discovered to hold for other phenomena such as partitioning between two liquid phases,[2,3] macromolecular conformational transitions,[4] enzyme activity,[5] protein denaturation,[6,7] viscosity, and critical micelle concentrations (CMCs) of surfactant solutions.[8−10] For a nonelectrolyte, the salting out effect is described by the Setschenow equation[11]

$$\ln f = -k_s C_{salt} \tag{1}$$

which describes how the activity coefficient f of an uncharged solute depends on the salt concentration C_{salt}. In this, k_s is an empirical, salt-specific Setschenow coefficient. We note that the Setschenow relation can be expressed in terms of natural or base 10 logarithms; for this work, we use the natural logarithm "ln". Also, regarding the level of accuracy to which we are working, it is not necessary to distinguish between molar and molal salt concentrations in eq 1 since the difference typically amounts to only a few percent for concentrations less than 1 M at room temperature and pressure. Moreover, since the Setschenow coefficients are arguably defined by their limiting values in eq 1 as C_{salt} tends to zero, this obviates the need to consider the densities of the salt solutions.

While the accurate determination of Setschenow coefficients relies on experimental methods, several models have been developed to predict the effect of a particular salt on a molecule in solution. Among these, an early attempt was made by Debye and MacAulay;[12] then, McDevit and Long later correlated k_s for benzene, as a solute, to the change in the volume of the solvent when salt is added;[13] Conway *et al.* used dielectric saturation to extend the theory to polyions;[14] and Masterton and Lee adopted a scaled particle theory to derive a general expression for the salt effect on benzene derivatives.[15] The use of empirical parameters and the relatively low accuracy of these models limit their use to only a few systems.[16] Wen-Hui *et al.* linked the Setschenow coefficient for sodium chloride to the Le Bas volume (V_{LB}) through a simple linear correlation, k_s = 0.0018 V_{LB},[17] while Gould used the intrinsic solubility of the solute.[18] Ni *et al.* showed how a linear correlation with the partition coefficient of the solute outperformed previous models,[19,20] but data availability limited the study to sodium chloride. More recently, Zhou[21] developed an electrostatic theory to describe the interaction of macromolecules with salt ions, showing good correlation with experimental data for protein solubility and stability. The salting out effect can be directly linked to an increase in surface tension, and Li *et al.* studied the change in solvation free energy of small molecules in the presence of different salts, concluding that Setschenow coefficients can be explained by the formation of nonpolar cavities in the salt solution and are not due to the direct interaction between solutes and ions.[22]

For surfactant solutions, the use of salts to control the CMC, micelle size and shape, and the correlated viscosity makes them an important formulation adjunct for many industrial

Received: January 6, 2022
Revised: March 3, 2022
Published: March 15, 2022

https://doi.org/10.1021/acs.jpcb.2c00101
J. Phys. Chem. B 2022, 126, 2308−2315

applications, such as home and personal care products. It is possible to rewrite eq 1 to describe the salt effect on the CMC of nonionic surfactants as[23]

$$\ln\left(\frac{\mathrm{CMC}}{\mathrm{CMC}_0}\right) = -k_s C_{\mathrm{salt}} \tag{2}$$

where CMC and CMC_0 are, respectively, the CMCs in aqueous salt solution and in pure water.

An attractive approach to surfactant formulation is to use computer simulations to supplement or even replace approximate theories and laborious experimental studies. Molecular dynamics (MD) has been extensively used to provide insights into the molecular details, for example, for protein−ion interactions of a single protein in a salt solution.[24−26] Studies have been carried out on the effects of salt on the water structure,[27,28] on the thermodynamics of hydration,[29] and on molecular association.[21,30] For example, Thomas and Elcock used MD to explore the correlation between the hydrophobic effect and water−ion hydrogen bonding using the Hofmeister series.[31] However, statistically meaningful sample sizes are required, and the small size of the systems accessible using MD can be a problem for uncertainty quantification.[32]

Due to the high computational costs of MD studies of surfactants, coarse-grained (CG) approaches are more usually deployed to explore micelle formation in surfactant solutions.[33] Salts have been incorporated in CGMD for both hard core and soft core repulsion methods.[34−41] The MARTINI force field describes hard core repulsion using a shifted Lennard-Jones potential, where the parameters depend on the bead type and are optimized using experimental solubility data.[42,43] Alternative methods for parameterization of soft core repulsion have recently been proposed.[37−39] Here, we use dissipative particle dynamics (DPD), a soft core CGMD methodology, which has been developed quite extensively for surfactant simulations. DPD was first introduced by Hoogerbrugge and Koelman[44] and later modified by Español and Warren[45] to satisfy Gibbs−Boltzmann statistics in a canonical *NVT* ensemble.[46] In DPD, a surfactant solution is modeled using soft particles called DPD beads. The solvent is represented by beads that represent two water molecules, salt ions are represented by adding charges to some of the water beads, and surfactant molecules are represented by a collection of connected DPD beads, which represent the various chemical subgroups. Dissipative and random forces between DPD beads provide a pairwise momentum-conserving thermostat,[45] but the main pairwise interactions are soft, short-range repulsions derived from

$$U_{ij}(r) = \frac{1}{2}a_{ij}\left(1 - \frac{r_{ij}}{R_{ij}}\right)^2 \qquad r_{ij} < R_{ij} \tag{3}$$

where a_{ij} is the amplitude of the interaction between beads i and j, r_{ij} is the distance between the two beads, and R_{ij} represents the range of the interaction (cutoff distance). It is through the a_{ij} and R_{ij} parameters that chemical specificity is captured, and recent systematic approaches provide transferable DPD force fields for which the same set of parameters and fragmentation strategy can be used to generate a bead representation of different molecules in different environments. For this work, we use a recent DPD force field which has been extensively validated for surfactant simulations.[47,48]

In the case of added salt, as well as for ionic surfactants, electrostatic interactions must also be included. Methods to implement electrostatics in DPD have received much attention in recent years, with the most common approach being the Ewald method.[33,38,49−53] However, in most studies, salt ions are represented simply as charged water beads,[37,54,55] and very little work has been done to parameterize the (non-electrostatic) short-range DPD repulsions with these charged beads despite this being an obvious target to capture ion-specific trends such as the Hofmeister series. Along these lines, Mayoral and Nahmad-Achar developed a parameterization for the repulsion amplitudes a_{ij} for the charged beads used in DPD based on the dependency of experimental Flory−Huggins χ parameters on salt concentration.[56] More recently, Nieto-Draghi and Rousseau proposed a parameterization procedure for electrolytes in an aqueous solution based on osmotic pressure,[57] but only ion−ion and ion−water bead interactions were investigated.

APPROACH

A systematic strategy to parameterize the interactions between salt beads and the DPD beads which represent the surfactant chemistry has not yet been proposed. Here, we present such a method based on matching to experimental Setschenow coefficients. First, we identify the key interactions between salts and surfactants which affect the CMC. Second, we demonstrate that DPD simulations of surfactants show the same log-linear dependence of the CMC on salt concentration as that reported in eq 2, which allows us to define the DPD equivalents to the empirical Setschenow coefficients. In the third step, we correlate these Setschenow coefficients with the repulsion parameters. Then, in the final step, we utilize the DPD length-scale mapping to match with experimentally determined Setschenow coefficients, providing a systematic basis for fixing the DPD interaction parameters between ions and surfactant beads.

Speciation and micelle formation in aqueous solutions is one of the most common targets of DPD surfactant simulations.[33,58] As already described, treating ions as charged water beads is a simple and convenient approach that has been used to obtain qualitatively good results for several systems.[38,39] However, this approach assumes that all ions are the same, which is in contrast to the experimental evidence for ion-specific trends. Table 1 shows that the experimental Setschenow coefficients that describe the effects of different salts on four nonionic surfactants, *n*-octanoyl-*N*-methylglucamine (MEGA8), *n*-nonanoyl-*N*-methylglucamine (MEGA9), *n*-octyl glucopyranoside (GLUCO8), and hexaethylene glycol monododecyl ether (C12E6), cover a wide range of values.

We selected two nonionic surfactants to use for initial parameterization.[60,61] DPD simulations perform most reliably for CMC values in the range 1−100 mM: if the CMC is too high, there is no distinction between submicellar aggregates and true micelles because of the overlap between the submicellar and micellar populations, and conversely, if the CMC is too low, the small number of free surfactants in solution leads to uncertainty.[38,47,62] Accordingly, we selected GLUCO8 and MEGA9, and the CG representations of these surfactants are shown in Figure 1. Table 1 includes Setschenow coefficients for some divalent ions (calcium, monohydrogen phosphate, sulfate, and carbonate). We include these for completeness since they may be useful in future work. To avoid complications arising from the nonideality of salt

https://doi.org/10.1021/acs.jpcb.2c00101
J. Phys. Chem. B 2022, 126, 2308−2315

Table 1. Experimental Setschenow Coefficients (k_s) for Nonionic Surfactants in Units of per Mole

	surfactants			
salts	MEGA8[57]	MEGA9[57]	GLUCO8[58]	C12E6[59]
LiCl	0.33	0.36	0.43	0.53
NaF	0.87	1.01		
NaCl	0.53	0.56	0.57	0.81
NaBr	0.37	0.45		
$NaNO_3$	0.30	0.37		
NaI	0.35	0.35		
NaSCN	0.29			
KCl	0.47	0.56		0.69
KBr	0.34	0.38		0.48
KI	0.26	0.30		0.30
CsCl	0.39			
$CaCl_2$	0.67			
Na_2HPO_4	1.20			
Na_2SO_3	1.38			
Na_2CO_3	1.53	1.79		
Na_2SO_4	1.59	1.85		

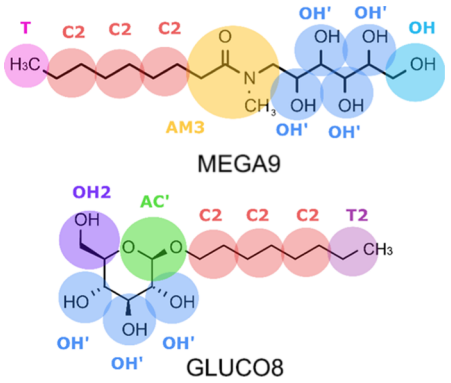

Figure 1. CG representations of MEGA9 and GLUCO8.

solutions containing multivalent ions, which may be significant, the present study focuses on the monovalent ions in Table 1.

SIMULATION DETAILS

DPD simulations were run for all the surfactant systems at different salt concentrations. The CG representation of the surfactants and the repulsion parameters for the beads were obtained from previous studies (Figure 1 and Table 2).[47,48] The cutoff distances in Table 2 were assigned as given in Anderson *et al.*[63] The repulsion amplitude between water beads is chosen conventionally as 25 k_BT so that the pressure of pure water in DPD units is 23.7.[63] In the model, the cutoff distance R_{ij} between water beads is defined as the DPD unit of length r_c, pure water is represented by water beads at a reduced density $\rho r_c^3 = 3$, and we suppose that each water bead represents N_m water molecules, where N_m is the so-called (water bead) mapping number.[64] To fit with the chosen DPD force field, we use $N_m = 2$.[45,62] If $V_m \approx 18 \times 10^{-6}$ m^3 is the molar volume of water, one can deduce that the volume of 1 mol of DPD volume elements $N_A r_c^3 = \rho r_c^3 \times N_m \times V_m \approx 0.108 \times 10^{-3}$ m^3 $\approx$ 0.108 litres, and hence, $r_c = 5.64$ Å. The DPD volume can be used to convert the number of salt beads (N_{salt}) to molar concentration units; namely, if the simulation box side is L, then

Table 2. DPD Parameters for All Pairwise Bead Interactions (Repulsion Amplitudes in Units of k_BT and Cutoff Distances in Units of r_c)

bead1	bead2	a_{ii}	a_{ij}	Δa_{ij}	R_{ij}
C2	C2	22.0			1.074
EO	EO	25.5			1.116
OH	OH	14.0			0.980
OH′	OH′	14.0			0.949
W	W	25.0			1.000
T	T	24.0			0.955
T2	T2	24.0			1.098
AC′	AC′	22.5			0.952
AM3	AM3	22.0			1.296
OH2	OH2	18.0			1.012
C2	EO		23.78	0.03	1.095
C2	OH		27.13	9.13	1.027
C2	W		45.54	21.95	1.037
C2	OH′		28.77	10.77	1.012
C2	AM3		21.83	−0.17	1.185
C2	AC′		18.17	−4.08	1.013
C2	T2		21.97	−1.03	1.086
OH′	AM3		11.00	−7.00	1.123
OH′	OH		13.86	−0.14	0.965
OH′	OH2		15.95	−0.05	0.981
OH′	AC′		19.42	1.17	0.951
OH′	T		28.85	9.85	0.952
OH′	T2		28.28	9.28	1.024
OH′	W		15.09	−4.41	0.975
EO	OH		18.17	1.33	1.048
EO	W		21.81	3.44	1.058
OH	W		18.17	1.33	0.990
OH	AM3		11.52	−6.48	1.138
OH2	AC′		17.42	−2.83	0.982
T	W		46.35	21.85	0.978
T	OH		27.49	8.49	0.968
T	C2		22.92	0.08	1.015
T	EO		24.18	1.05	1.036
T	AM3		22.32	−0.68	1.126
W	OH2		22.20	0.70	1.006
W	AC′		7.74	−16.01	0.976
W	AM3		13.20	−10.30	1.148
W	T2		45.44	20.94	1.049
T2	AC′		17.32	−5.93	1.025
T2	OH2		27.59	6.59	1.024

$$\frac{C_{salt}}{\text{Molar}} = \frac{N_{salt}}{(L/r_c)^3 (N_A r_c^3/\text{litres})} \quad (4)$$

Molecularly bonded beads are held together with a harmonic spring potential

$$U(r) = \frac{1}{2} k_b (r_{ij} - r_0)^2$$

where $k_b = 150\ k_BT$, and a three-body angular potential

$$U(\theta) = \frac{1}{2} k_a (\theta_{ij} - \theta_0)^2$$

where $k_a = 5\ k_BT$. The equilibrium distance r_0 and the equilibrium angle θ_0 were assigned using the method previously reported.[48]

Simulations were performed in a cubic box of side $L = 30\ r_c$ with the total number of beads equal to 81,000. They were run

https://doi.org/10.1021/acs.jpcb.2c00101
J. Phys. Chem. B 2022, 126, 2308−2315

for 4×10^6 steps with a time step of 0.01 in DPD time units, starting from a random initial configuration. By measuring the diffusion of small molecules in a related DPD model with a comparable level of coarse graining, Sevink and Fraaije determined the underlying DPD time unit ≈ 50 ps, so the time step in our simulations should correspond to about 0.5 ps,[65] making the total simulation run time 1−2 μs. This timescale is long enough for micelles to form and to equilibrate. Simulations were run in the isothermal−isobaric ensemble (NPT) using the standard velocity Verlet integration algorithm.[66] Trajectory files were collected every 10^3 time steps. Simulations were performed using DL_MESO (version 2.7).[67] Post-simulation trajectory analysis was performed using a combination of the UMMAP analysis tool[68] and bespoke analysis scripts.

DPD simulations were run at 4, 5, and 6 wt % for all surfactants. The aggregation number distribution is a plot of population $P(N)$ *versus* aggregation number (N), and this distribution can be used to discriminate between monomers and submicellar aggregates (designated free surfactant) and stable micelles as described in previous studies.[47,48] By plotting this distribution, one discerns a region depleted in stable micelles, which allows the definition of a value of N_{cut} to separate the free surfactants ($N < N_{cut}$) from micelles ($N > N_{cut}$). For each simulation, the minimum in $P(N)$ from the aggregation number distribution was used as N_{cut}. The CMC was calculated as the total concentration of free surfactants after reaching the equilibrium (typically after 5×10^5 steps). The values of CMC did not vary significantly with surfactant concentration, and the average values are quoted.

As a starting point, each salt ion was represented by a positive bead or a negative bead, with the same R_{ij} and a_{ij} as that of water (*i.e.*, as charged water beads), and then, the a_{ij} values were varied to study the effect on the calculated CMC of the surfactant. The Slater-type charge smearing for the electrostatic interactions proposed by González-Melchor *et al.* was adopted.[69] For a pair of particles, the electrostatic interaction potential can be written as

$$U_{ij}^{El} = \frac{\Gamma q_i q_j}{4\pi r_{ij}}(1 - (1 + \beta^* r_{ij})\, e^{-2\beta^* r_{ij}}) \quad (5)$$

where r_{ij} is the distance between particles i and j, q_i and q_j are the ion valences, and β^* is the Slater smearing parameter (set to be equal to 0.929 r_c^{-1}). The strength of the interaction is governed by $\Gamma = e^2/(k_B T \varepsilon_0 \varepsilon_r r_c)$, which is a dimensionless electrostatic coupling parameter. Following Vaiwala *et al.*[70] and Anderson *et al.*,[38] we assume a uniform relative dielectric permittivity of $\varepsilon_r = 78.3$ and $T = 298$ K, resulting in $\Gamma = 15.94$ for $r_c = 5.64$ Å. The k-vector cutoff in the k-space was set as 5 r_c^{-1}. Changing the cutoff from 1 r_c^{-1} to 10 r_c^{-1} did not show any effect on the CMC value of neutral surfactants. The real-space Ewald cutoff was set as 3.0 r_c.

RESULTS AND DISCUSSION

First, the effect of changing the values of a_{ij} for interactions between salt ions and other beads was investigated though the effect on the CMC. Figure 2 shows the relationship between the CMC and the a_{ij} parameters for ion−water (blue), ion−tail (green), and ion−head group (yellow) interactions. Beads T, T2, and C2 were considered part of the hydrophobic tail, and beads AM3, OH, OH′, OH2, and AC′ were considered part of the hydrophilic head group. Figure 2 compares the results for

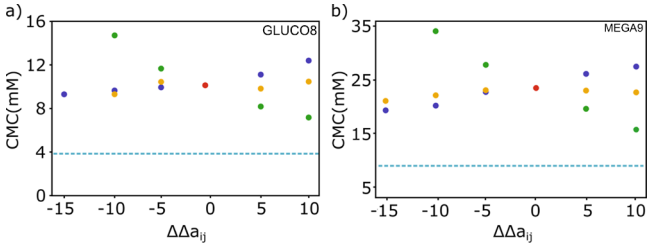

Figure 2. Calculated CMC value plotted as a function of the change in the repulsion parameter Δa_{ij} relative to the water−water value for interactions of the ion beads with water (blue), hydrophilic head groups (yellow), and the hydrophobic tail (green) for (a) GLUCO8 and (b) MEGA9. The red point represents the CMC values obtained using the standard water a_{ij} values (*i.e.*, $\Delta a_{ij} = 0$). The salt concentration was 1 M, and the dotted line shows the experimental CMC value obtained for the surfactant in a 1 M solution of NaCl.

MEGA9 and GLUCO8 obtained using a salt concentration of 1 M with the experimental values (dotted line). The plots show that the ion−tail interactions have a much bigger effect in decreasing the CMC values than the ion−head and ion−water interactions and that the best way to approach values closer to the experimental values is by further increasing the repulsion parameter for the ion−tail interactions. Therefore, we focused our attention on these interaction parameters, which is in line with the conclusions obtained by Mukerjee in his studies on C_xE_y surfactants, where the contribution of the hydrophilic head to k_s for neutral surfactants was reported to be negligible.[23]

Ion−tail a_{ij} values were screened from 35 k_BT to 150 k_BT for both the anion (a_{ij^-}) and cation (a_{ij^+}), and the CMC values were calculated for both surfactants. The result for GLUCO8 with $a_{ij^+} = a_{ij^-}$ reported in Figure 3a shows a nonlinear

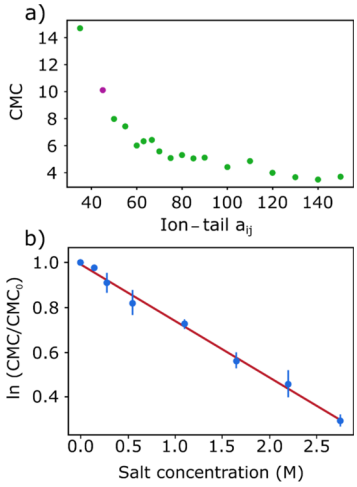

Figure 3. (a) Relationship between the CMC value and the ion−tail a_{ij} parameter for GLUCO8. (b) Linear correlation between ln(CMC/CMC$_0$) and salt concentration for $a_{ij} = 100\ k_BT$.

relationship, which reaches a plateau around $a_{ij} = 140\ k_BT$. The CMC value increases sharply for small a_{ij} values, which is consistent with the negative k_s values observed for polyoxyethylenes.[71] The effect of salt concentration on the CMC value was then studied. The CMC values were averaged from three independent simulation runs with surfactant concentrations of 4, 5, and 6 wt %. These simulations were repeated using different ion−tail a_{ij} values and for a range of salt

https://doi.org/10.1021/acs.jpcb.2c00101
J. Phys. Chem. B 2022, 126, 2308−2315

concentrations between 0 and 2.75 M. Figure 3b shows an example of the results. In all cases, a clear log-linear relationship was found between CMC and salt concentration.

Slopes of plots of the CMC values obtained in DPD simulations *versus* salt concentration were used to calculate values of k_s as a function of the ion−tail repulsion parameters used in the simulations. The relationship between the calculated values of k_s and the values of a_{ij^-} and a_{ij^+} for the anion−tail and cation−tail interactions is shown in Figure 4 for

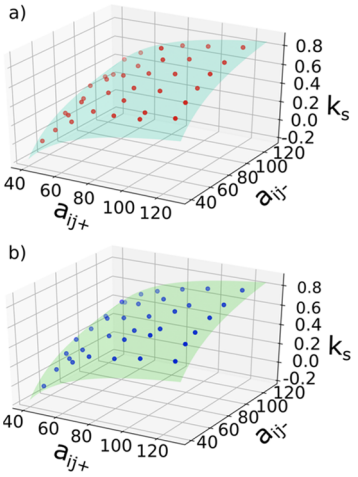

Figure 4. Relationship between the values of k_s obtained from DPD simulations and the repulsion parameters for the cation−tail (a_{ij^+}) and anion−tail (a_{ij^-}) interactions for (a) MEGA9 and (b) GLUCO8. The shaded surfaces were obtained by fitting to eq 6.

GLUCO8 and MEGA9. The surfaces colored in green in Figure 4 are the best fit for the following relationship

$$k_s = A\left(\frac{1}{a_{ij^+}} + \frac{1}{a_{ij^-}}\right) + B \quad (6)$$

where A and B are constants that depend on the surfactant (Table 3).

Table 3. A and B Parameters Used to Describe Different Surfactants in Eq 6[a]

	surfactants			
parameter	MEGA8	MEGA9	GLUCO8	C12E6
A	−29.42	−30.03	−29.04	−52.32
B	1.24	1.32	1.29	2.09

[a]Sum of the square of residuals from fitting: MEGA8 0.00053, MEGA9 0.00037, C12E6 0.00123, and GLUCO8 = 0.00067 M^{-1}.

The interesting property of eq 6 is that the terms that describe interactions with the anion and the cation appear separately so that a salt can be described simply as the sum of the individual effects of the anion and the cation on the CMC. Having established values of A and B for GLUCO8 and MEGA9, the experimentally determined values of k_s measured for these surfactants in different salt solutions can be used in conjunction with eq 6 to derive the repulsion parameters required to describe the individual ions. The ion−tail repulsion parameters for lithium, sodium, and potassium cations and for chloride, bromide, and iodide anions were obtained by fitting the experimental values of k_s for GLUCO8 and MEGA9 in Table 1 to eq 6 using a generalized reduced gradient nonlinear method. Having established repulsion parameters for a range of different anions and cations, the experimentally determined values of k_s measured for different surfactants in the corresponding salt solutions can be used in conjunction with eq 6 to derive the constants A and B required to describe the surfactants. The parameters for MEGA8 and C12E6 were obtained by fitting the experimental values of k_s in Table 1 to eq 6, and the results are shown in Table 3. The repulsion parameters for the ions listed in Table 4 were then optimized

Table 4. Ion−Tail Repulsion Parameters for Cations and Anions

cation	anion	a_{ij^+}	a_{ij^-}
Li^+		51	
Na^+		72	
K^+		64	
Cs^+		55	
	Cl^-		94
	Br^-		66
	I^-		55
	NO_3^-		56
	SCN^-		54

by using the experimental values of k_s for all four surfactants in eq 6 and the values of A and B in Table 3. The parameters in Tables 3 and 4 provide an excellent description of the experimental k_s values for all four surfactants in solutions of 10 different salts (Figure 5). The results suggest that eq 6 can be

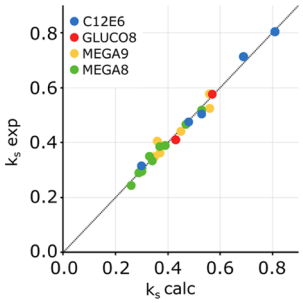

Figure 5. Comparison of the calculated values of k_s with the experimental values for four different surfactants in 10 different salt solutions (in blue, C12E6; in red, GLUCO8; in yellow, MEGA9; and in green, MEGA8). R^2 = 0.98.

used to predict the effects of salts on other surfactants, provided sufficient experimental data are available to estimate the A and B parameters for the surfactant (Table 5).

The parameters for thiocyanate and caesium ions in Table 4 were obtained from single measurements and should be considered less reliable than the other values. The parameter for the fluoride ion could not be determined by changing the ion−tail repulsion parameter because the a_{ij} value required was too large. It is clear that fluoride has the highest repulsion parameter of all of the anions, but some other interactions must be involved to account for the behavior of these systems, such as a specific interaction with the surfactant or a direct effect on the counterion. The trends in a_{ij} values are $F^- > Cl^- > Br^- > NO_3^- > I^- > SCN^-$ for anions and $Na^+ > K^+ > Cs^+ > Li^+$ for cations. With the exception of K^+, which precedes Na^+ in

https://doi.org/10.1021/acs.jpcb.2c00101
J. Phys. Chem. B 2022, 126, 2308−2315

Table 5. Comparison of Calculated and Experimental Setschenow Coefficients (k_s) in Units of per Mole

surfactant	cation	anion	k_s exp	k_s calc	error
C12E6	Li^+	Cl^-	0.53	0.50	0.03
	Na^+	Cl^-	0.81	0.80	0.01
	K^+	Cl^-	0.69	0.71	−0.02
	K^+	Br^-	0.48	0.48	0.00
	K^+	I^-	0.30	0.32	−0.02
GLUCO8	Na^+	Cl^-	0.57	0.58	−0.01
	Li^+	Cl^-	0.43	0.41	0.02
MEGA8	Li^+	Cl^-	0.33	0.35	−0.02
	Na^+	Cl^-	0.53	0.52	0.01
	Na^+	Br^-	0.37	0.39	−0.02
	Na^+	NO_3^-	0.30	0.31	−0.01
	Na^+	I^-	0.30	0.30	0.00
	Na^+	SCN^-	0.29	0.29	0.00
	K^+	Cl^-	0.47	0.47	0.00
	K^+	Br^-	0.34	0.33	0.01
	K^+	I^-	0.26	0.24	0.02
	Cs^+	Cl^-	0.39	0.39	0.00
MEGA9	Li^+	Cl^-	0.36	0.41	−0.05
	Na^+	Cl^-	0.56	0.58	−0.02
	Na^+	Br^-	0.45	0.44	0.01
	Na^+	NO_3^-	0.37	0.36	0.01
	Na^+	I^-	0.35	0.35	0.00
	K^+	Cl^-	0.56	0.52	0.04
	K^+	Br^-	0.38	0.39	−0.01
	K^+	I^-	0.30	0.30	0.00

the cation series, both sequences match the Hofmeister series.[1,72]

CONCLUSIONS

A method for calculating the interaction parameters between salt ion beads and surfactant beads for DPD simulations has been developed. DPD simulations show that the calculated CMC values depend largely on the ion−tail repulsion parameter, and to a first approximation, the other interactions in the system can be ignored. When CMC values were calculated as a function of the concentration of salt ion beads, the results were found to reproduce the empirical Setschenow relationship, and the calculated values of the Setschenow constant k_s therefore provide a direct connection with an experimentally determined parameter that describes the interaction of ions with surfactants in aqueous salt solutions. A general equation has been derived that describes the Setschenow constant k_s in terms of the repulsion parameter for the cation−tail interaction, the repulsion parameter for the anion−tail interaction, and two surfactant parameters A and B. By fitting the calculated values of k_s to the experimental values, it was possible to derive A and B parameters for four different surfactants and repulsion parameters for a range of different ions. The resulting parameters provide accurate descriptions the experimental behavior of these surfactant systems in 10 different salt solutions. This result provides a general approach for the parameterization of repulsion parameters for charged species in DPD simulations.

Our observation that the Setschenow trends can be captured in the present model by tuning the ion−tail interactions supports the notion that the Setschenow coefficients are a measure of the solvent "quality" in these systems. Thus, our results underscore the idea that, in this context, the Hofmeister series reflects changes in the hydrophobic effect acting on the surfactant tails.[73] We emphasize in this respect that apart from the ion−tail interactions in Table 4, the ions are otherwise treated as charged water beads (*cf.*, the "W" beads given in Table 2). This means for instance that trends in ion activities are *not* reproduced in the present model. This could be solved by combining the approach with, for example, the parameterization strategy for ion−ion and ion−water interactions proposed by Nieto-Draghi and Rousseau,[57] which could then be extended to include multivalent ions. Further work will also be required to extend the approach to ionic surfactants and to test the effect of changes in the nature of the hydrocarbon tail. The case of polyions (polyelectrolytes) is also of considerable interest; however, these are often involved with very specific effects such as adsorption onto surfactant micelles[74] and would require separate treatment.

AUTHOR INFORMATION

Corresponding Author

Christopher A. Hunter − *Department of Chemistry, University of Cambridge, Cambridge CB2 1EW, U.K.*; orcid.org/0000-0002-5182-1859; Email: herchelsmith.orgchem@ch.cam.ac.uk

Authors

Ennio Lavagnini − *Department of Chemistry, University of Cambridge, Cambridge CB2 1EW, U.K.*

Joanne L. Cook − *Unilever R&D Port Sunlight, Bebington CH63 3JW, U.K.*

Patrick B. Warren − *Unilever R&D Port Sunlight, Bebington CH63 3JW, U.K.; STFC Hartree Centre, Sci-Tech Daresbury, Warrington WA4 4AD, U.K.*

Complete contact information is available at: https://pubs.acs.org/10.1021/acs.jpcb.2c00101

Notes

The authors declare the following competing financial interest(s): PBW and JLC declare a substantive (> $10k) stock holding in Unilever PLC. All other authors declare no competing financial interest.

ACKNOWLEDGMENTS

We thank the Engineering and Physical Sciences Research Council and Unilever PLC for financial support.

REFERENCES

(1) Hofmeister, F. Zur Lehre von Der Wirkung Der Salze. *Arch. Exp. Pathol. Pharmakol.* **1888**, *24*, 247−260.

(2) Hao, L.; Nan, Y.; Liu, H.; Hu, Y. Salt Effects on Aqueous Cationic/Anionic Surfactant Two-Phase Regions. *J. Dispersion Sci. Technol.* **2006**, *27*, 271−276.

(3) Ferreira, L.; Madeira, P. P.; Mikheeva, L.; Uversky, V. N.; Zaslavsky, B. Effect of Salt Additives on Protein Partition in Polyethylene Glycol−Sodium Sulfate Aqueous Two-Phase Systems. *Biochim. Biophys. Acta, Proteins Proteomics* **2013**, *1834*, 2859−2866.

(4) Piculell, L.; Nilsson, S. Effects of Salts on Association and Conformational Equilibria of Macromolecules in Solution. In *Surfactants and Macromolecules: Self-Assembly at Interfaces and in Bulk*; Lindman, B., Rosenholm, J. B., Stenius, P., Eds.; Steinkopff: Darmstadt, 1990; pp 198−210.

(5) Warren, J. C.; Cheatum, S. G. Effect of Neutral Salts on Enzyme Activity and Structure. *Biochemistry* **1966**, *5*, 1702−1707.

(6) Pegram, L. M.; Wendorff, T.; Erdmann, R.; Shkel, I.; Bellissimo, D.; Felitsky, D. J.; Record, M. T. Why Hofmeister Effects of Many

Salts Favor Protein Folding but Not DNA Helix Formation. *Proc. Natl. Acad. Sci. U.S.A.* **2010**, *107*, 7716−7721.
(7) Nandi, P. K.; Robinson, D. R. Effects of Salts on the Free Energy of the Peptide Group. *J. Am. Chem. Soc.* **1972**, *94*, 1299−1308.
(8) Penfield, K. A Look behind the Salt Curve: The Link between Rheology, Structure, and Salt Content in Shampoo Formulations. *Int. J. Cosmet. Sci.* **2005**, *27*, 300.
(9) Penfield, K.; Co, A.; Leal, G. L.; Colby, R. H.; Giacomin, A. J. A Look Behind the Salt Curve: An Examination of Thickening Mechanisms in Shampoo Formulations. *AIP Conf. Proc.* **2008**, *1027*, 899−901.
(10) Arleth, L.; Bergström, M.; Pedersen, J. S. Small-Angle Neutron Scattering Study of the Growth Behavior, Flexibility, and Intermicellar Interactions of Wormlike SDS Micelles in NaBr Aqueous Solutions. *Langmuir* **2002**, *18*, 5343−5353.
(11) Setschenow, J. Über die Konstitution der Salzlösungen auf Grund ihres Verhaltens zu Kohlensäure. *Z. Phys. Chem.* **1889**, *4*, 117−125.
(12) Debye, P.; MacAulay, I. Das elektrische Feld der Ionen und die Neutralsalzwirkung. *Phys. Z.* **1925**, *26*, 22−29.
(13) McDevit, W. F.; Long, F. A. The Activity Coefficient of Benzene in Aqueous Salt Solutions. *J. Am. Chem. Soc.* **1952**, *74*, 1773−1777.
(14) Conway, B. E.; Desnoyers, J. E.; Smith, A. C.; Dainton, F. S. On the Hydration of Simple Ions and Polyions. *Philos. Trans. R. Soc. London, Ser. A* **1964**, *256*, 389−437.
(15) Masterton, W. L.; Lee, T. P. Salting Coefficients from Scaled Particle Theory. *J. Phys. Chem.* **1970**, *74*, 1776−1782.
(16) Wen-Hui, X.; Jing-Zhe, S.; Xi-Ming, X. Studies on the Activity Coefficient of Benzene and Its Derivatives in Aqueous Salt Solutions. *Thermochim. Acta* **1990**, *169*, 271−286.
(17) Reid, R. C.; Prausnitz, J. M.; Poling, B. E. *The Properties of Gases and Liquids*; McGraw Hill Book Co.: New York, NY, United States, 1987.
(18) Gould, P. L. Salt Selection for Basic Drugs. *Int. J. Pharm.* **1986**, *33*, 201−217.
(19) Ni, N.; El-Sayed, M. M.; Sanghvi, T.; Yalkowsky, S. H. Estimation of the Effect of NaCl on the Solubility of Organic Compounds in Aqueous Solutions. *J. Pharm. Sci.* **2000**, *89*, 1620−1625.
(20) Ni, N.; Yalkowsky, S. H. Prediction of Setschenow Constants. *Int. J. Pharm.* **2003**, *254*, 167−172.
(21) Zhou, H.-X. Interactions of Macromolecules with Salt Ions: An Electrostatic Theory for the Hofmeister Effect. *Proteins: Struct., Funct., Bioinf.* **2005**, *61*, 69−78.
(22) Li, L.; Fennell, C. J.; Dill, K. A. Small Molecule Solvation Changes Due to the Presence of Salt Are Governed by the Cost of Solvent Cavity Formation and Dispersion. *J. Chem. Phys.* **2014**, *141*, 22D518.
(23) Mukerjee, P. Salt Effects on Nonionic Association Colloids. *J. Phys. Chem.* **1965**, *69*, 4038−4040.
(24) Horinek, D.; Serr, A.; Bonthuis, D. J.; Boström, M.; Kunz, W.; Netz, R. R. Molecular Hydrophobic Attraction and Ion-Specific Effects Studied by Molecular Dynamics. *Langmuir* **2008**, *24*, 1271−1283.
(25) Maity, H.; Muttathukattil, A. N.; Reddy, G. Salt Effects on Protein Folding Thermodynamics. *J. Phys. Chem. Lett.* **2018**, *9*, 5063−5070.
(26) Karplus, M.; McCammon, J. A. Molecular Dynamics Simulations of Biomolecules. *Nat. Struct. Biol.* **2002**, *9*, 646−652.
(27) Chang, T.-M.; Dang, L. X. Recent Advances in Molecular Simulations of Ion Solvation at Liquid Interfaces. *Chem. Rev.* **2006**, *106*, 1305−1322.
(28) Riemenschneider, J.; Holzmann, J.; Ludwig, R. Salt Effects on the Structure of Water Probed by Attenuated Total Reflection Infrared Spectroscopy and Molecular Dynamics Simulations. *ChemPhysChem* **2008**, *9*, 2731−2736.
(29) Kalra, A.; Tugcu, N.; Cramer, S. M.; Garde, S. Salting-In and Salting-Out of Hydrophobic Solutes in Aqueous Salt Solutions. *J. Phys. Chem. B* **2001**, *105*, 6380−6386.
(30) Ray, A.; Nemethy, G. Effects of Ionic Protein Denaturants on Micelle Formation by Nonionic Detergents. *J. Am. Chem. Soc.* **1971**, *93*, 6787−6793.
(31) Thomas, A. S.; Elcock, A. H. Molecular Dynamics Simulations of Hydrophobic Associations in Aqueous Salt Solutions Indicate a Connection between Water Hydrogen Bonding and the Hofmeister Effect. *J. Am. Chem. Soc.* **2007**, *129*, 14887−14898.
(32) Grossfield, A.; Patrone, P. N.; Roe, D. R.; Schultz, A. J.; Siderius, D. W.; Zuckerman, D. M. Best Practices for Quantification of Uncertainty and Sampling Quality in Molecular Simulations. *Living J. Comput. Mol. Sci.* **2018**, *1*, 5067.
(33) Taddese, T.; Anderson, R. L.; Bray, D. J.; Warren, P. B. Recent Advances in Particle-Based Simulation of Surfactants. *Curr. Opin. Colloid Interface Sci.* **2020**, *48*, 137−148.
(34) Wang, S.; Larson, R. G. Coarse-Grained Molecular Dynamics Simulation of Self-Assembly and Surface Adsorption of Ionic Surfactants Using an Implicit Water Model. *Langmuir* **2015**, *31*, 1262−1271.
(35) Liu, D.; Liu, F.; Zhou, W.; Chen, F.; Wei, J. Molecular Dynamics Simulation of Self-Assembly and Viscosity Behavior of PAM and CTAC in Salt-Added Solutions. *J. Mol. Liq.* **2018**, *268*, 131−139.
(36) Van Liefferinge, F.; Krammer, E.-M.; Sengupta, D.; Prévost, M. Lipid Composition and Salt Concentration as Regulatory Factors of the Anion Selectivity of VDAC Studied by Coarse-Grained Molecular Dynamics Simulations. *Chem. Phys. Lipids* **2019**, *220*, 66−76.
(37) Tang, X.; Zou, W.; Koenig, P. H.; McConaughy, S. D.; Weaver, M. R.; Eike, D. M.; Schmidt, M. J.; Larson, R. G. Multi-Scale Modeling of the Effects of Salt and Perfume Raw Materials on the Rheological Properties of Commercial Thread-like Micellar Solutions. *J. Phys. Chem. B* **2017**, *121*, 2468−2485.
(38) Anderson, R. L.; Bray, D. J.; Del Regno, A.; Seaton, M. A.; Ferrante, A. S.; Warren, P. B. Micelle Formation in Alkyl Sulfate Surfactants Using Dissipative Particle Dynamics. *J. Chem. Theory Comput.* **2018**, *14*, 2633−2643.
(39) Panoukidou, M.; Wand, C. R.; Del Regno, A.; Anderson, R. L.; Carbone, P. Constructing the Phase Diagram of Sodium Laurylethoxysulfate Using Dissipative Particle Dynamics. *J. Colloid Interface Sci.* **2019**, *557*, 34−44.
(40) Bore, S. L.; Kolli, H. B.; Kawakatsu, T.; Milano, G.; Cascella, M. Mesoscale Electrostatics Driving Particle Dynamics in Nonhomogeneous Dielectrics. *J. Chem. Theory Comput.* **2019**, *15*, 2033−2041.
(41) Kolli, H. B.; de Nicola, A.; Bore, S. L.; Schäfer, K.; Diezemann, G.; Gauss, J.; Kawakatsu, T.; Lu, Z.-Y.; Zhu, Y.-L.; Milano, G.; Cascella, M. Hybrid Particle-Field Molecular Dynamics Simulations of Charged Amphiphiles in an Aqueous Environment. *J. Chem. Theory Comput.* **2018**, *14*, 4928−4937.
(42) Marrink, S. J.; Risselada, H. J.; Yefimov, S.; Tieleman, D. P.; de Vries, A. H. The MARTINI Force Field: Coarse Grained Model for Biomolecular Simulations. *J. Phys. Chem. B* **2007**, *111*, 7812−7824.
(43) Marrink, S. J.; de Vries, A. H.; Mark, A. E. Coarse Grained Model for Semiquantitative Lipid Simulations. *J. Phys. Chem. B* **2004**, *108*, 750−760.
(44) Hoogerbrugge, P. J.; Koelman, J. M. V. A. Simulating Microscopic Hydrodynamic Phenomena with Dissipative Particle Dynamics. *Europhys. Lett.* **1992**, *19*, 155−160.
(45) Español, P.; Warren, P. B. Statistical Mechanics of Dissipative Particle Dynamics. *Europhys. Lett.* **1995**, *30*, 191.
(46) Daan, F.; Berend, S. *Understanding Molecular Simulation*; Academic Press, 2002.
(47) Lavagnini, E.; Cook, J. L.; Warren, P. B.; Williamson, M. J.; Hunter, C. A. A Surface Site Interaction Point Method for Dissipative Particle Dynamics Parametrization: application to Alkyl Ethoxylate Surfactant Self-Assembly. *J. Phys. Chem. B* **2020**, *124*, 5047−5055.
(48) Lavagnini, E.; Cook, J. L.; Warren, P. B.; Hunter, C. A. Translation of Chemical Structure into Dissipative Particle Dynamics

https://doi.org/10.1021/acs.jpcb.2c00101
J. Phys. Chem. B 2022, 126, 2308−2315

Parameters for Simulation of Surfactant. *J. Phys. Chem. B* **2021**, *125*, 3942−3952.
(49) Ewald, P. P. Die Berechnung Optischer Und Elektrostatischer Gitterpotentiale. *Ann. Phys.* **1921**, *369*, 253−287.
(50) Groot, R. D. Electrostatic Interactions in Dissipative Particle Dynamics—Simulation of Polyelectrolytes and Anionic Surfactants. *J. Chem. Phys.* **2003**, *118*, 11265−11277.
(51) Mao, R.; Lee, M.-T.; Vishnyakov, A.; Neimark, A. V. Modeling Aggregation of Ionic Surfactants Using a Smeared Charge Approximation in Dissipative Particle Dynamics Simulations. *J. Phys. Chem. B* **2015**, *119*, 11673−11683.
(52) Sanders, S. A.; Sammalkorpi, M.; Panagiotopoulos, A. Z. Atomistic Simulations of Micellization of Sodium Hexyl, Heptyl, Octyl, and Nonyl Sulfates. *J. Phys. Chem. B* **2012**, *116*, 2430−2437.
(53) Eslami, H.; Khani, M.; Müller-Plathe, F. Gaussian Charge Distributions for Incorporation of Electrostatic Interactions in Dissipative Particle Dynamics: Application to Self-Assembly of Surfactants. *J. Chem. Theory Comput.* **2019**, *15*, 4197−4207.
(54) Goodarzi, F.; Zendehboudi, S. Effects of Salt and Surfactant on Interfacial Characteristics of Water/Oil Systems: Molecular Dynamic Simulations and Dissipative Particle Dynamics. *Ind. Eng. Chem. Res.* **2019**, *58*, 8817−8834.
(55) Wan, M.; Gao, L.; Fang, W. Implicit-Solvent Dissipative Particle Dynamics Force Field Based on a Four-to-One Coarse-Grained Mapping Scheme. *PLoS One* **2018**, *13*, No. e0198049.
(56) Mayoral, E.; Nahmad-Achar, E. Study of Interfacial Tension between an Organic Solvent and Aqueous Electrolyte Solutions Using Electrostatic Dissipative Particle Dynamics Simulations. *J. Chem. Phys.* **2012**, *137*, 194701.
(57) Nieto-Draghi, C.; Rousseau, B. Thermodynamically Consistent Force Field for Coarse-Grained Modeling of Aqueous Electrolyte Solution. *J. Phys. Chem. B* **2019**, *123*, 2424−2431.
(58) Español, P.; Warren, P. B. Perspective: Dissipative Particle Dynamics. *J. Chem. Phys.* **2017**, *146*, 150901.
(59) Miyagishi, S.; Okada, K.; Asakawa, T. Salt Effect on Critical Micelle Concentrations of Nonionic Surfactants, *N*-Acyl-*N*-Methyl-glucamides (MEGA-N). *J. Colloid Interface Sci.* **2001**, *238*, 91−95.
(60) Mukerjee, P.; Chan, C. C. Effects of High Salt Concentrations on the Micellization of Octyl Glucoside: Salting-Out of Monomers and Electrolyte Effects on the Micelle−Water Interfacial Tension1. *Langmuir* **2002**, *18*, 5375−5381.
(61) Carale, T. R.; Pham, Q. T.; Blankschtein, D. Salt Effects on Intramicellar Interactions and Micellization of Nonionic Surfactants in Aqueous Solutions. *Langmuir* **1994**, *10*, 109−121.
(62) Johnston, M. A.; Swope, W. C.; Jordan, K. E.; Warren, P. B.; Noro, M. G.; Bray, D. J.; Anderson, R. L. Toward a Standard Protocol for Micelle Simulation. *J. Phys. Chem. B* **2016**, *120*, 6337−6351.
(63) Anderson, R. L.; Bray, D. J.; Ferrante, A. S.; Noro, M. G.; Stott, I. P.; Warren, P. B. Dissipative Particle Dynamics: Systematic Parametrization Using Water-Octanol Partition Coefficients. *J. Chem. Phys.* **2017**, *147*, 094503.
(64) Groot, R. D.; Rabone, K. L. Mesoscopic Simulation of Cell Membrane Damage, Morphology Change and Rupture by Nonionic Surfactants. *Biophys. J.* **2001**, *81*, 725−736.
(65) Sevink, G. J. A.; Fraaije, J. G. E. M. Efficient Solvent-Free Dissipative Particle Dynamics for Lipid Bilayers. *Soft Matter* **2014**, *10*, 5129−5146.
(66) Verlet, L. Computer "Experiments" on Classical Fluids. I. Thermodynamical Properties of Lennard-Jones Molecules. *Phys. Rev.* **1967**, *159*, 98−103.
(67) Seaton, M. A.; Anderson, R. L.; Metz, S.; Smith, W. DL_MESO: Highly Scalable Mesoscale Simulations. *Mol. Simul.* **2013**, *39*, 796−821.
(68) Bray, D. J.; Del Regno, A.; Anderson, R. L. UMMAP: a statistical analysis software package for molecular modelling. *Mol. Simul.* **2020**, *46*, 308−322.
(69) González-Melchor, M.; Mayoral, E.; Velázquez, M. E.; Alejandre, J. Electrostatic Interactions in Dissipative Particle Dynamics Using the Ewald Sums. *J. Chem. Phys.* **2006**, *125*, 224107.
(70) Vaiwala, R.; Jadhav, S.; Thaokar, R. Electrostatic Interactions in Dissipative Particle Dynamics Ewald-like Formalism, Error Analysis, and Pressure Computation. *J. Chem. Phys.* **2017**, *146*, 124904.
(71) Doren, A.; Goldfarb, J. Electrolyte Effects on Micellar Solutions of Nonionic Detergents. *J. Colloid Interface Sci.* **1970**, *32*, 67−72.
(72) Hyde, A. M.; Zultanski, S. L.; Waldman, J. H.; Zhong, Y.-L.; Shevlin, M.; Peng, F. General Principles and Strategies for Salting-Out Informed by the Hofmeister Series. *Org. Process Res. Dev.* **2017**, *21*, 1355−1370.
(73) Kronberg, B. The hydrophobic effect. *Curr. Opin. Colloid Interface Sci.* **2016**, *22*, 14−22.
(74) Hansson, P.; Lindman, B. Surfactant-polymer interactions. *Curr. Opin. Colloid Interface Sci.* **1996**, *1*, 604−613.

https://doi.org/10.1021/acs.jpcb.2c00101
J. Phys. Chem. B 2022, 126, 2308−2315